Am J Transl Res 2026;18(3):2659-2673
www.ajtr.org /ISSN:1943-8141/AJTR0169980

Original Article

Decursin ameliorates diabetic kidney disease by attenuating renal epithelial-mesenchymal transition via inhibition of the PI3K/Akt pathway

Yuxin Xiong[1,2], Xiaoling Wang[2], Jiaoli Chen[2], Qian Feng[3], Xian Li[4], Ke Yang[5], Ying Yang[1,2]

[1]Department of Endocrinology, Kunming Medical University, Kunming, Yunnan, China; [2]Department of Endocrinology, The Affiliated Hospital of Yunnan University, Kunming, Yunnan, China; [3]Department of Clinical Examination, The Affiliated Hospital of Yunnan University, Kunming, Yunnan, China; [4]School of Medicine, Dali University, Dali, Yunnan, China; [5]Ruijin Hospital Shanghai Jiaotong University School of Medicine, Shanghai, China

Received November 13, 2025; Accepted February 9, 2026; Epub March 25, 2026; Published March 30, 2026

Abstract: Objective: This study aims to elucidate the therapeutic mechanisms of Decursin (DE) against diabetic kidney disease (DKD), focusing on its effects on renal epithelial-mesenchymal transition (EMT) and the underlying signaling pathways. Methods: A streptozotocin (STZ)-induced DKD model was established in rats and treated with DE for 12 weeks. Metabolic and renal function indices were assessed using blood and urine samples, while kidney tissues were subjected to histopathological examination. Network pharmacology and disease database analyses were employed to predict the core target genes of DE in DKD. The predicted targets and EMT-related processes were further validated using human renal tubular epithelial cells (HK2) under high glucose (HG) or transforming growth factor-beta 1 (TGF-β1) stimulation. The expression of core target proteins and EMT markers was evaluated by Western blotting in both in vivo and in vitro settings. Results: DE treatment significantly ameliorated biochemical parameters and renal EMT in DKD rats. Network analysis identified 16 potential target genes, with MMP-9, ESR1, PTGS2, AR, and CTNNB1 ranked as the top five core genes. Molecular docking and protein-protein interaction analysis further prioritized MMP-9, PI3K, and Akt as the most promising hub targets of DE. Consistently, Western blot analysis confirmed that DE markedly downregulated the expression of PI3K, phosphorylated Akt (p-Akt), and EMT-related proteins (including MMP-9, N-cadherin, and α-SMA) both in DKD rat kidneys and in HG- or TGF-β1-stimulated HK2 cells. Furthermore, the PI3K inhibitor LY294002 produced similar anti-EMT effects, thereby confirming the involvement of the PI3K/Akt pathway in the action of DE. Conclusion: Integrating experimental and network pharmacology approaches, this study demonstrates that DE alleviates renal EMT in DKD by inhibiting the PI3K/Akt signaling pathway, providing preliminary evidence for future studies.

Keywords: Diabetic kidney disease, Decursin, network pharmacology, epithelial-mesenchymal transition

Introduction

Diabetic kidney disease (DKD) is a serious chronic microvascular complication of diabetes and has become the leading cause of chronic kidney disease (CKD) and end-stage renal disease (ESRD) worldwide [1, 2]. The rising global incidence of diabetes has been paralleled by a rapid increase in the prevalence of DKD [3]. It is well established that DKD patients have a significantly higher risk of fatal cardiovascular events compared to diabetic patients without kidney involvement [4]. Although intensive glycemic control can reduce diabetes-related complications through metabolic memory, including the development of DKD, it does not effectively slow the progression to ESRD in patients with established DKD [5, 6]. Renal fibrosis represents the final common pathway in the pathophysiology of DKD, in which epithelial-mesenchymal transition (EMT) plays an important role [7, 8]. EMT is a cellular process strongly associated with hyperglycemia and contributes significantly to mesenchymal stromal deposition and renal fibrosis in DKD [9, 10]. The occurrence of EMT in DKD patients is closely linked to multiple factors, including abnormal blood glucose levels, transforming

https://doi.org/10.62347/TPVW2438

growth factor-β1 (TGF-β1) expression, overactivation of the phosphatidylinositol 3-kinase/protein kinase B (PI3K/Akt) signaling pathway, and inflammatory responses [11, 12]. Among these, the PI3K/Akt pathway is notably associated with extracellular matrix (ECM) accumulation and EMT, both of which are correlated with renal fibrosis [13, 14]. Growing evidence further supports the essential role for the PI3K/Akt signaling pathway in regulating EMT during the progression of DKD [15].

Decursin (DE), a coumarin compound derived from the roots of *Angelica Gigas* Naka (also known as Dang Gui in Chinese), possesses well-documented pharmacological properties, including anti-inflammatory, antioxidant and anti-anemia effects [16-18]. In our previous study, we demonstrated that DE alleviates pathological proliferation and angiogenesis in diabetic retinopathy by inhibiting VEGFR2 expression [19]. Additionally, DE has been reported to inhibit cervical tumor growth by regulating the PI3K/Akt signaling pathway [20]. Despite extensive research into its pharmacological activities, it remains unclear whether DE influences PI3K/AKT pathway-associated EMT in DKD.

In this study, we evaluated the renal effects of DE in a DKD rat model and observed that DE significantly ameliorated EMT and biochemical parameters. Using network pharmacology and disease databases, we screened for potential core target genes and pathways involved in DE's action against DKD. These findings were further validated through protein-protein interaction (PPI) analysis, molecular docking, and Western blot assays both in vivo and in vitro. Overall, our results indicate that DE improves renal EMT in DKD by inhibiting the PI3K/Akt pathway, thereby providing a basis for its potential clinical application.

Materials and methods

Animals and ethical approval

Male Sprague-Dawley rats aged 10 weeks (n=50, body weight 220-250 g) were obtained from the Wuhan Myhalic Biotechnology Co., Ltd. The Wuhan Myhalic Biotechnology Co., Ltd. Animal Ethics Committee approved all experimental procedures (License No. HLK-20241109). These procedures followed the guidelines set forth in the NIH's Guide for the Care and Use of Laboratory Animals (Publication No. 85-23, revised 1996).

Under specific pathogen-free conditions, the rats were housed at 24±2°C with a 12-hour light/dark cycle. They had free access to food and water throughout the study. Prior to experimentation, all animals underwent a 7-day acclimatization and were then randomly assigned to either a normal control group (n=10) or a model group (n=40). Diabetes in the model group was induced by a single intraperitoneal injection of freshly prepared streptozotocin (STZ, 50 mg/kg, Solarbio, S8050, China) in cold citrate buffer (pH 4.5). Control animals received an equal-volume injection of normal saline. Fasting blood glucose levels were tested weekly after the third injection using a glucose meter (OneTouch Verio Vue, LifeScan, USA). Four weeks after STZ administration, the urinary albumin-to-creatinine ratio (UACR) was assessed with biochemical analyzers (BN II System, Siemens, Germany and Architechtc-16000, Abbott, USA). Rats with sustained hyperglycemia (blood glucose > 16.7 mmol/L) and elevated UACRs were considered to have DKD and were subsequently randomized into a DKD group (n=18, after excluding 2 non-responsive rats) and a DKD+DE group (n=19, after excluding 1 non-responsive rat). All groups were fed standard rodent chow. The DKD+DE group was administered 20 mg/kg DE (Ache Action DEol Complex, Now Foods, USA) [21] by oral gavage daily for 12 weeks, while the DKD and control groups received an equivalent volume of saline. Blood glucose and body weight were recorded weekly throughout the experimental period.

Biochemical analysis

At the end of the treatment period, all animals were fasted overnight, weighed the following day, and 6 hour urine samples were obtained for the measurement of the UACR. All animals were then anesthetized and euthanized via intraperitoneal injection of an appropriate does of sodium pentobarbital. Blood samples were taken from the abdominal aorta, followed by cervical dislocation. Serum levels of glucose, blood urea nitrogen (BUN), uric acid (UA), serum creatinine (SCr), triglycerides (TG), and total cholesterol (TC) were determined using an automatic biochemistry analyzer (Roche, Germany and UniCel DxI 800 Access, USA). The

kidneys were immediately harvested, weighed, fixed in 10% neutral buffered formalin or snap-frozen in liquid nitrogen for storage at -80°C for further experiments.

Histological analysis

To prepare for histological examination, kidney samples were paraffin-embedded and cut into 5 μm sections. These sections underwent staining with hematoxylin and eosin (H&E), periodic acid-Schiff (PAS), and Masson's trichrome staining kits (DC0032, Leagene Biotechnology, China) according to the manufacturer's instructions. For visualization, the stained slides were digitally scanned with CaseViewer 2.4 software (3DHISTECH. Ltd., Hungary) and region of interest were selected at 200× magnification. Subsequent quantitative analysis of the images was conducted using Image-Pro Plus 6.0 software (Media Cybernetics, USA).

Determination of disease-related and drug-target genes

Disease-associated genes for diabetic kidney disease (DKD) were compiled by integrating related targets from multiple databases, including GeneCards, TTD, DrugBank, and OMIM. Meanwhile, potential targets of DE were sourced from the Traditional Chinese Medicine Systems Pharmacology Database and Analysis Platform (TCMSP) and the STITCH database.

Construction of protein-protein interaction (PPI) network and identification of core genes

Construction of the PPI network was performed on the STRING platform (https://string-db.org) with a confidence threshold set above 0.4 for interactions. The resulting network was then imported into Cytoscape software (version 3.8.2) [22] for visualization and further topological analysis. Identification of core genes was based on their connectivity within the network, with the selection of the top five highest-degree nodes as hub genes using the degree algorithm from the CytoHubba plugin.

Molecular docking

Molecular docking was performed to evaluate the binding affinity of DE to potential therapeutic targets in DKD, with particular focus on the PI3K/Akt pathway - a key signaling cascade in DKD pathogenesis [23], as well as MMP-9, which is closely associated with epithelial-mesenchymal transition (EMT) [24]. The three-dimensional (3D) structure of the target protein was obtained from the Protein Data Bank (PDB, https://www.rcsb.org/). Water molecules and native ligands were removed from the protein's structure. AutoDock Tools (version 4.2) [25] was used for hydrogen addition and charge assignment of the proteins. Next, the two-dimensional (2D) chemical structure of DE was retrieved from the TCMSP database and subsequently prepared for docking using AutoDock Tools, including charge assignment and identification of rotatable bonds. Finally, molecular docking simulations and binding energy calculations were performed using AutoDock Vina (version 1.1.2) [26]. A more negative ΔG value generally indicates a more stable ligand-protein complex and a higher probability of interaction [27]. The resulting docking poses were visualized and analyzed using PyMOL software (version 2.4.1).

Cell culture and treatment

Human proximal tubular epithelial cells (HK2 cells; BNCC100395, Bena Culture Collection, China) were cultured in low-glucose (LG) Dulbecco's Modified Eagle Medium (DMEM, 5.5 mM glucose; C3113-0500, VivaCell, China) supplemented with 10% fetal bovine serum (FBS, C04001-050, VivaCell, China), 100 U/mL penicillin, and 100 μg/mL streptomycin (C3421, VivaCell, China). Cells were maintained at 37°C in a humidified incubator containing 5% CO_2. The HK-2 cell line was selected because it reliably undergoes EMT under high glucose and TGF-β1 stimulation, making it a suitable in vitro model for studying this mechanism [28]. TGF-β1 is a well-established cytokine for inducing epithelial-EMT [29], it was used in this study to generate an EMT-positive control model.

HK2 cells were then assigned to the following treatment groups under different culture conditions: (1) LG group: cultured in LG DMEM; (2) HG group: cultured in HG DMEM (40 mM glucose); (3) LG+TGF-β1 group: cultured in LG DMEM supplemented with 10 ng/mL TGF-β1 (PeproTech, China); (4) HG+DE group: cultured in HG DMEM (40 mM glucose) with 25 μM DE (CFN98509, ChemFaces, China).

In order to investigate the role of the PI3K/Akt pathway, 20 μM LY294002 (MCE, China) was

administered to the LG+TGF-β1 and HG groups. This inhibitor concentration, chosen based on prior literature [30], was added 1 hour after the initial treatments. All groups were incubated under the described conditions for 24 hours, after which cells were harvested and lysed for the detection of downstream signaling molecules by western blotting.

MTS assay

To identify a therapeutically effective yet non-cytotoxic concentration of DE, a cell proliferation assay was conducted using the MTS method (G3580, Promega, USA). HK-2 cells were seeded into 96-well plates at 6×10^3 cells per well. They were subsequently exposed to varying doses of DE (0, 25, 50, 100 μM) and/or TGF-β1 (0, 5, 10 ng/mL; AF-100-21C, PeproTech) for either 24 or 48 hours. After incubation, 20 μL of MTS reagent was added per well, followed by a 3-hour incubation at 37°C. The absorbance at 490 nm was then recorded with a microplate reader. All treatments were performed with five technical replicates, and the complete experiment was independently replicated three times.

Western blot analysis

Proteins were extracted from kidney tissues and HK2 cells using RIPA buffer (R0010, Solarbio, China) according to the manufacturer's instructions, and the protein concentrations were quantified with a bicinchoninic acid (BCA) protein assay kit (T9300A, Takara, Japan). Equal amounts of protein from each experimental group were separated by sodium dodecyl sulfate-polyacrylamide gel electrophoresis (SDS-PAGE) and transferred onto polyvinylidene difluoride (PVDF) membranes. The membranes were blocked with 5% non-fat milk (232100, BD Life Science, USA) for 2 hours at room temperature and then incubated overnight at 4°C with the following primary antibodies: anti-N-cadherin (1:3000, 22018-1-AP, Proteintech, China), anti-PI3K (1:800, PTM-6358, PTM BIO, China), anti-MMP-9 (1:1000, 10375-2-AP, Proteintech, China), anti-p-Akt (1:1000, PTM-6735, PTM BIO, China), anti-Akt (1:1000, PTM-6071, PTM BIO, China), anti-α-SMA (1:2000, 14395-1-AP, Proteintech, China) and anti-β-actin (1:2000, PTM-5028, PTM BIO, China). Following four rinses in TBST (Tris-buffered saline with 0.1% Tween-20), the membranes were probed with an HRP-linked secondary antibody (1:5000 dilution; SA00001-2, Proteintech, China) for 1.5 hours at room temperature. For signal detection, an enhanced chemiluminescence (ECL) kit (180-501, Tanon, China) was applied. The chemiluminescent signals were then captured using a ChemiDoc XRS+ imaging system (Bio-Rad, USA). Finally, a densitometric analysis of the protein bands was performed with ImageJ software (version 1.51j8, NIH, USA) to quantify band intensities. To evaluate the role of EMT, we employed Western blotting to detect key EMT markers, including the mesenchymal cell marker N-cadherin, α-SMA and MMP-9 [31, 32].

Statistical analyses

Statistical analysis was conducted using GraphPad Prism 9.0 (GraphPad Software, Inc., San Diego, CA, USA). Data presentation and analysis followed these criteria: all values from a minimum of three independent experiments are mean ± SD; group differences were evaluated via one-way ANOVA with Bonferroni post hoc correction for multiple comparisons; and a *P*-value below 0.05 was considered statistically significant.

Results

DE ameliorates biochemical parameters and renal pathology in DKD rats

Rats treated with STZ exhibited typical diabetic symptoms, including polydipsia, polyphagia and polyuria, accompanied by a significant increase in the UACR four weeks after STZ administration (Supplementary Figure 1). Both the DKD and DKD+DE groups had significantly increased blood glucose, KW/BW ratio, and TG levels but showed a significant decline in body weight compared to the control group. The DKD group displayed significantly higher UACR and BUN levels than the control group, and these increases were significantly attenuated following DE treatment. Similarly, TC levels were elevated in the DKD group compared to the control group, and DE administration effectively reversed this change. No significant differences in UA or SCr were observed among the three groups (**Table 1**). Examination of H&E-stained sections revealed significantly milder renal tubular hypertrophy and glomerular enlargement in the DE-treated diabetic rats relative to

Table 1. Effects of DE on physical and biochemical parameters in experimental rats

	Control	DKD	DKD+DE
Glucose (mmol/L)	6.002±0.553	30.01±8.063*	29.99±8.113*
Body weight (g)	496.4±55.03	371.0±18.11*	378.1±16.59*
KW/BW (mg/g)	0.675±0.074	1.354±0.251*	1.365±0.217*
UACR (mg/mmol)	4.615±1.856	22.29±8.271*	13.97±2.847*,#
BUN (mmol/L)	12.96±0.678	18.39±1.923*	15.71±2.561*,#
UA (μmol/L)	77.13±8.935	76.40±24.35	76.20±23.82
SCr (μmol/L)	34.86±9.406	31.40±6.736	28.10±5.626
TG (mmo/L)	0.448±0.132	2.612±1.372*	1.883±1.018*
TC (mmol/L)	1.491±0.439	2.533±0.622*	1.989±0.238#

Data were presented as mean ± SD (n=10-15). Abbreviations: DKD, diabetic kidney disease; DE, Decursin; UACR, urinary albumin to creatinine ratio; BUN, blood urea nitrogen; UA, uric acid; SCr, serum creatinine; and KW/BW, kidney weight to body weight ratio; *P < 0.05 versus the control group, #P < 0.05 versus the DKD group.

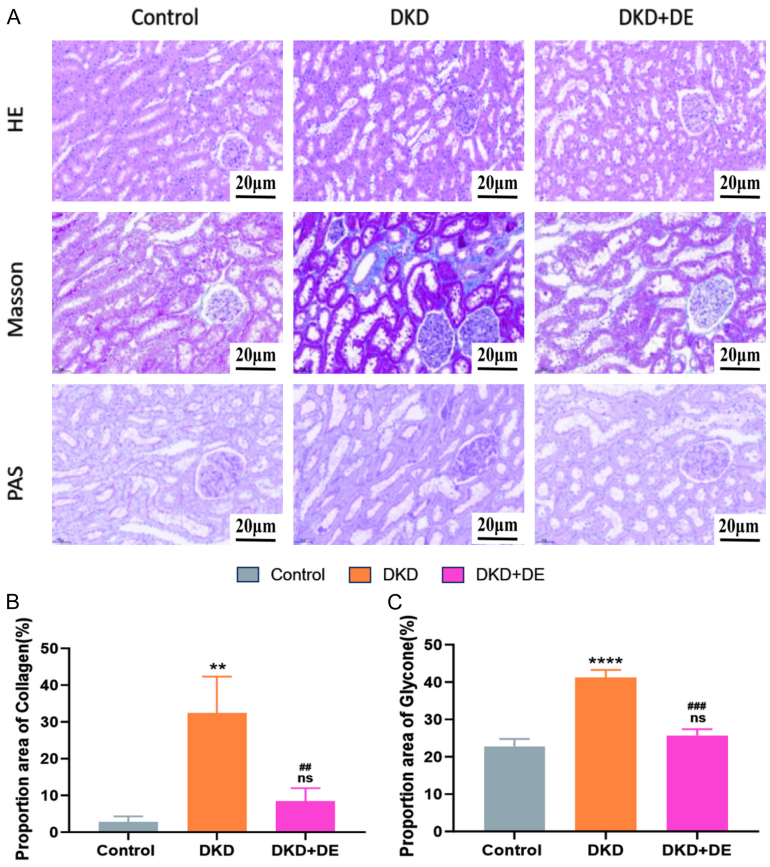

Figure 1. DE ameliorates renal fibrosis in DKD rats. A. Representative images of kidney sections stained with H&E, Masson and PAS. Original magnification: ×200; scale bar =20 μm. B, C. Quantitative analysis of the collagen-positive area (Masson staining) and glycogen-positive area (PAS staining). Data are presented as mean ± SD (n=3 independent experiments). Statistical analysis was performed using one-way ANOVA followed by post-hoc comparisons in GraphPad Prism 9.0. ns, not significance; ns, **P < 0.01, ****P < 0.0001 versus the control group. ##P < 0.01 and ###P < 0.001 versus the DKD group. DKD, Diabetic Kidney Disease; DE, Decursin.

the untreated DKD group (**Figure 1A**). In contrast, kidneys from DKD rats exhibited greater glycogen accumulation, as indicated by PAS staining. Similarly, increased collagen deposition (evident as blue staining) was observed in this group compared to controls using Masson's trichrome staining. Both pathological features were significantly mitigated after 12 weeks of DE intervention (**Figure 1B**, **1C**). These findings suggest that DE alleviates renal fibrosis, reduces UACR and BUN, and improves dyslipidemia in DKD rats through mechanisms independent of glycemic or bodyweight modulation.

Identification of potential target and PPI network for DE in DKD

We retrieved 22 candidate targets for DE by searching the TCMSP and STITCH databases (Supplementary Table 1). Separately, we collected disease-associated genes for DKD from four public databases: GeneCards (3,487 targets), TTD (23), DrugBank

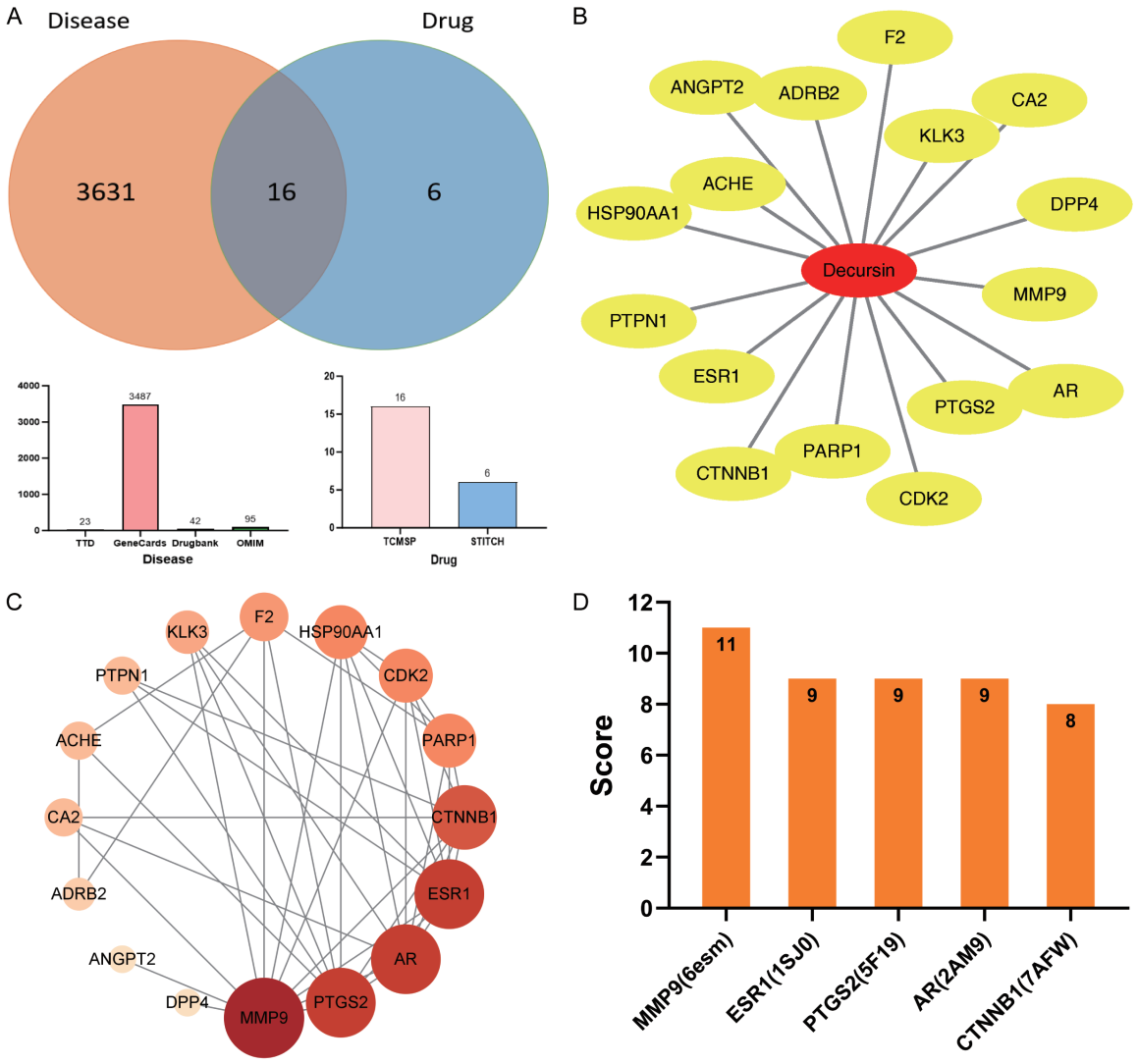

Figure 2. Identification of hub targets of DE for DKD through network analysis. A. Venn diagram showing the overlap between DKD-related genes and DE target genes. Data were collected from TTD, GeneCards, DrugBank, OMIM, TCMSP, and STITCH databases. B. Drug-target interaction network of DE. C. Protein-protein interaction (PPI) network of the 16 overlapping genes. D. The top five genes ranked by degree centrality using the CytoHubba plugin in Cytoscape. DKD, Diabetic Kidney Disease; DE, Decursin.

(42), and OMIM (95) (Supplementary Table 1). Intersection analysis revealed 16 overlapping genes between the DE-target and disease-target sets (**Figure 2A**). A drug-target interaction network was subsequently constructed based on those 16 genes (**Figure 2B**). To explore their functional relationships and identify core targets, these overlapping genes were used to construct PPI network via the STRING database, resulting in a network of 16 nodes and 43 edges (**Figure 2C**). Finally, applying the degree algorithm through the CytoHubba plugin within Cytoscape, the top five hub genes - MMP-9, ESR1, PTGS2, AR, and CTNNB1 - were pinpointed as the central therapeutic targets of DE against DKD (**Figure 2D**).

Molecular docking analysis of DE with PI3K/Akt and EMT-related targets

Molecular docking shown DE exhibited strong binding affinity to key proteins implicated in DKD (**Figure 3**). Notably, DE showed favorable binding energies with PI3K (-8.2 kcal/mol) and Akt (-7.4 kcal/mol) (**Figure 3A-C**). Among the five core targets identified from the PPI network, DE displayed the strongest binding

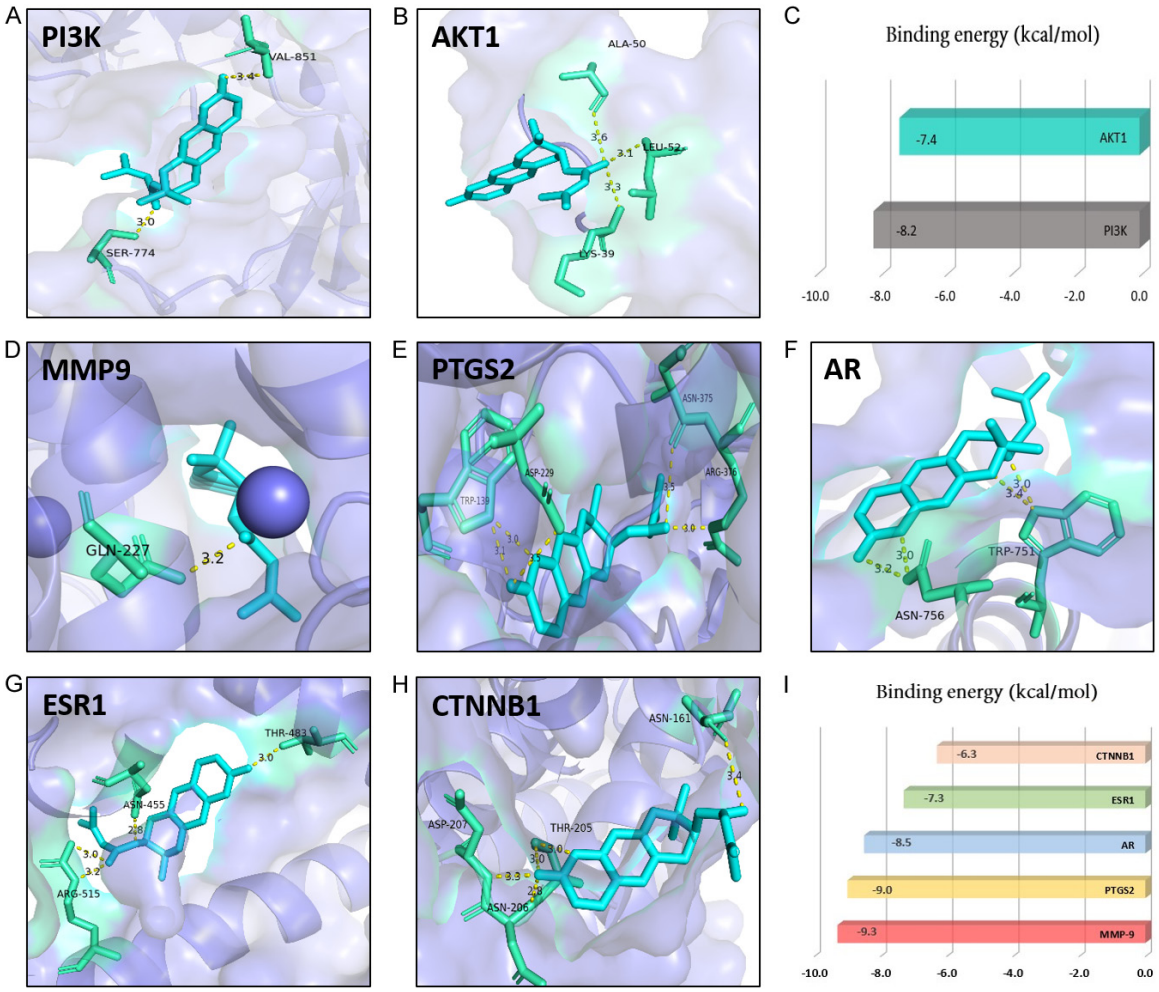

Figure 3. Molecular docking analysis of DE with core target proteins. A, B. Predicted binding modes of DE within the active sites of PI3K and Akt, respectively. C. Calculated binding energies of DE with PI3K and Akt. D-H. Binding poses of DE with the top five candidate targets (MMP-9, PTGS2, AR, ESR1, and CTNNB1) identified from the PPI network. I. Binding energies of DE with the aforementioned five target proteins. DE, Decursin; ESR1, estrogen receptor alpha.

potential to MMP-9, with a binding energy of -9.3 kcal/mol (**Figure 3D-I**). The binding energies for the other core targets (ESR1, PTGS2, AR, and CTNNB1) are listed in **Figure 3E-I**. These results indicate that DE can stably bind to the active sites of PI3K, Akt, and MMP-9, supporting their roles as potential direct targets in the therapeutic action of DE against DKD.

DE ameliorates renal EMT and suppresses the PI3K/Akt pathway in DKD rats

We examined key proteins related to EMT (MMP-9, N-cadherin, and α-SMA) and the PI3K/Akt pathway. The results demonstrated that the elevated expression of MMP-9, N-cadherin, and α-SMA in DKD rats was were significantly counteracted by DE intervention (**Figure 4A-D**). Similarly, the increased levels of PI3K and the p-Akt/Akt ratio observed in the DKD group were also effectively reduced following DE administration (**Figure 4E-G**). In summary, these data confirm that DE treatment alleviates renal EMT and inhibits PI3K/Akt signaling in a rat model of DKD.

DE attenuates high glucose-induced EMT and suppresses the PI3K/Akt pathway in HK2 cells

An MTS assay indicated that DE at low concentrations did not significantly affect HK2 cell viability, whereas 100 μM DE markedly reduced cell survival (Supplementary Figure 2).

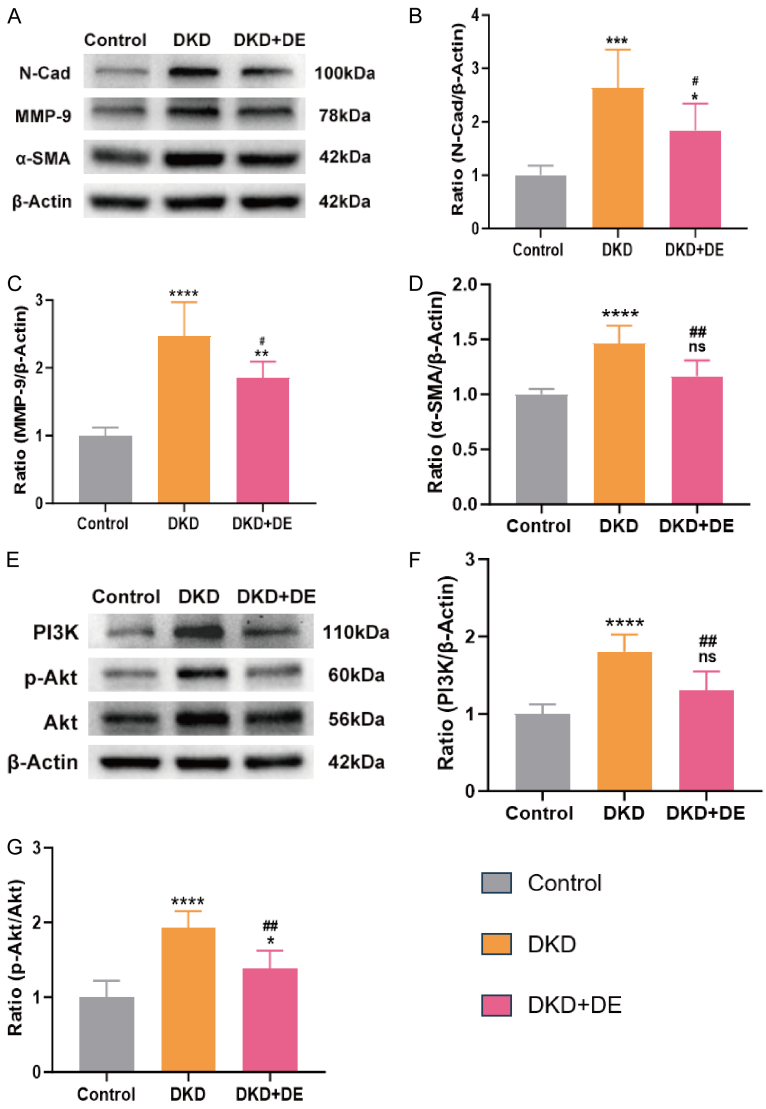

Figure 4. DE attenuates renal EMT and inhibits the PI3K/Akt pathway in DKD rats. A. Representative Western blot images of N-cadherin, MMP-9 and α-SMA in rat kidneys. B-D. Quantitative analysis of N-cadherin, MMP-9, and α-SMA protein levels, respectively. E. Representative Western blot images of PI3K, p-Akt, and Akt. F, G. Quantitative analysis of PI3K protein level and the p-Akt/Akt ratio, respectively. Data are presented as mean ± SD (n=6 rats per group) from three independent experiments. Statistical significance was determined by one-way ANOVA with post-hoc comparisons using GraphPad Prism 9.0. *P < 0.05, **P < 0.01, ***P < 0.001, ****P < 0.0001 versus the control group; #P < 0.05, ##P < 0.01 versus the DKD group. DKD, diabetic kidney disease; DE, Decursin; ns, not significant. EMT, epithelial-mesenchymal transition; DKD, Diabetic Kidney Disease.

Consequently, 25 μM DE was selected for subsequent experiments. Then, we further validated the effects of DE on EMT induced by TGF-β1 and HG. Morphological analysis revealed that cells in the LG group maintained a typical epithelial cobblestone-like shape (Supplementary Figure 3). As shown in **Figure 5**, HG exposure significantly upregulated the protein levels of the EMT-related markers MMP-9, N-cadherin, and α-SMA, an effect similar to that of TGF-β1. DE treatment significantly reversed these increases (**Figure 5A-D**). Furthermore, both HG and TGF-β1 stimulation elevated the expression of PI3K and the p-Akt/Akt. These inductions were also significantly suppressed by DE (**Figure 5E-G**). These results demonstrate that DE alleviates HG-induced EMT and inhibits the activation of the PI3K/Akt pathway in vitro.

DE attenuates HG-induced EMT through inhibiting the PI3K/Akt pathway

Exposure of HK2 cells to HG significantly increased the expression of the EMT-related proteins (PI3K, N-cadherin, and α-SMA) and activated the PI3K/Akt pathway as evidenced by elevated PI3K levels and Akt phosphorylation. DE treatment effectively suppressed these HG-induced changes. To further determine whether the PI3K/Akt pathway mediates the anti-EMT effect of DE, we used the specific PI3K inhibitor LY294002. Inhibition of by LY294002 abolished the upregulation of MMP-9, N-cadherin, and α-SMA induced by either TGF-β1 or HG. Notably, DE treatment produced a similar inhibitory effect (**Figure 6A-D**). Consistently, LY249200 also blocked the HG and TGF-β1-induced increases in PI3K expression and Akt phosphorylation, mirroring the action of DE (**Figure 6E-G**). These findings demonstrate that DE alleviates HG-induced EMT through a mechanism involving inhibition of the PI3K/Akt signaling pathway.

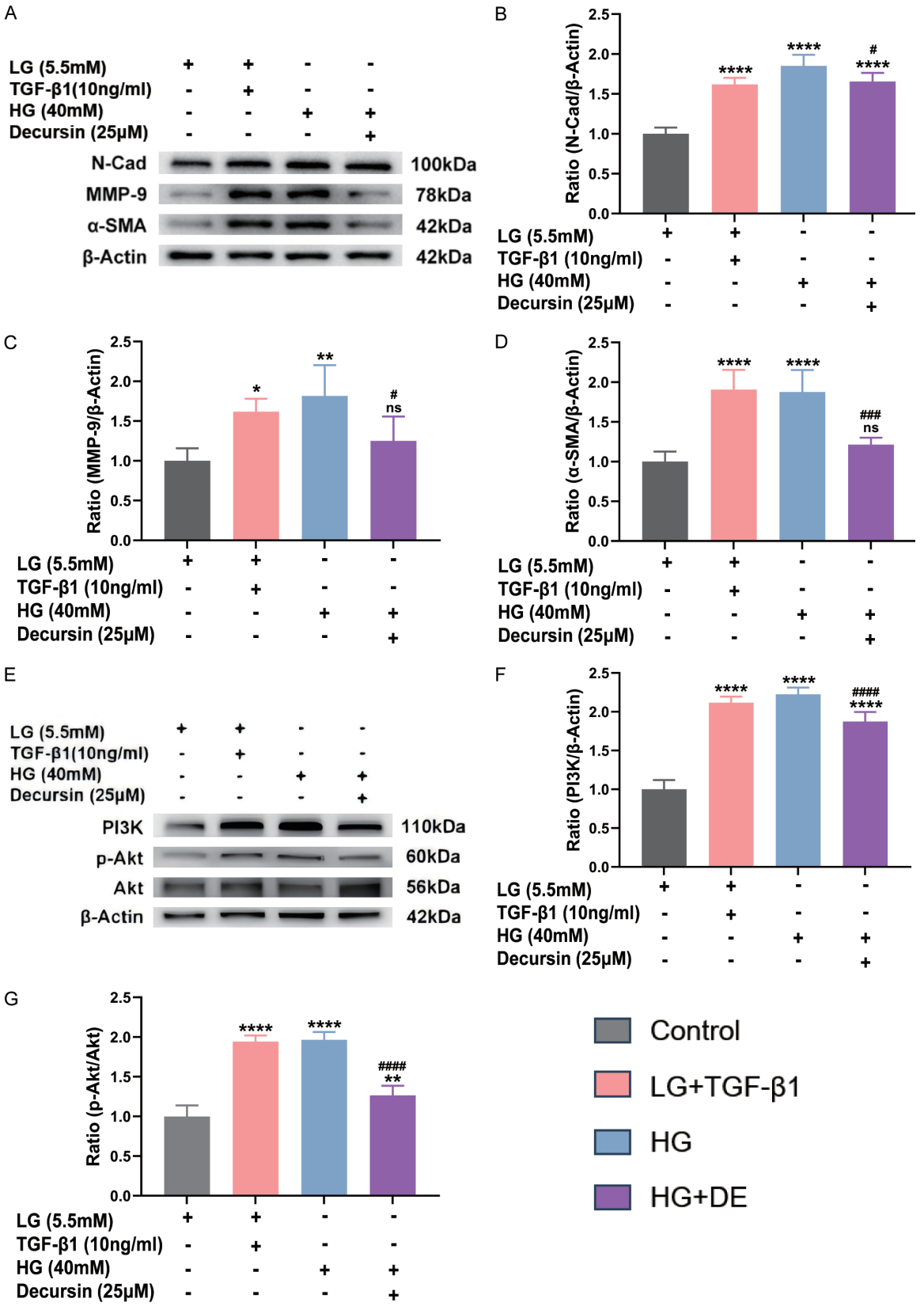

Figure 5. DE attenuates EMT and inhibits PI3K/Akt signaling in HG-induced HK2 cells. A. Western blotting images of N-cadherin, MMP-9, and α-SMA in HK2 cells cultured under LG, LG+TGF-β1, HG, and HG+DE conditions. B-D. Quantification analysis of N-cadherin, MMP-9, and α-SMA protein levels, respectively. E. Western blotting images of PI3K, p-Akt, and Akt. F, G. Quantification analysis of PI3K protein level and the p-Ak/Akt ratio, respectively. Data

are presented as mean ± SD from three independent experiments (n=3). Statistical significance was determined by one-way ANOVA with post-hoc comparisons using GraphPad Prism 9.0. *P < 0.05, **P < 0.01, ****P < 0.0001 versus the LG group; #P < 0.05, ###P < 0.001, ####P < 0.0001 versus the HG group. ns, not significant. LG, low-glucose; HG, high glucose; EMT, epithelial-mesenchymal transition.

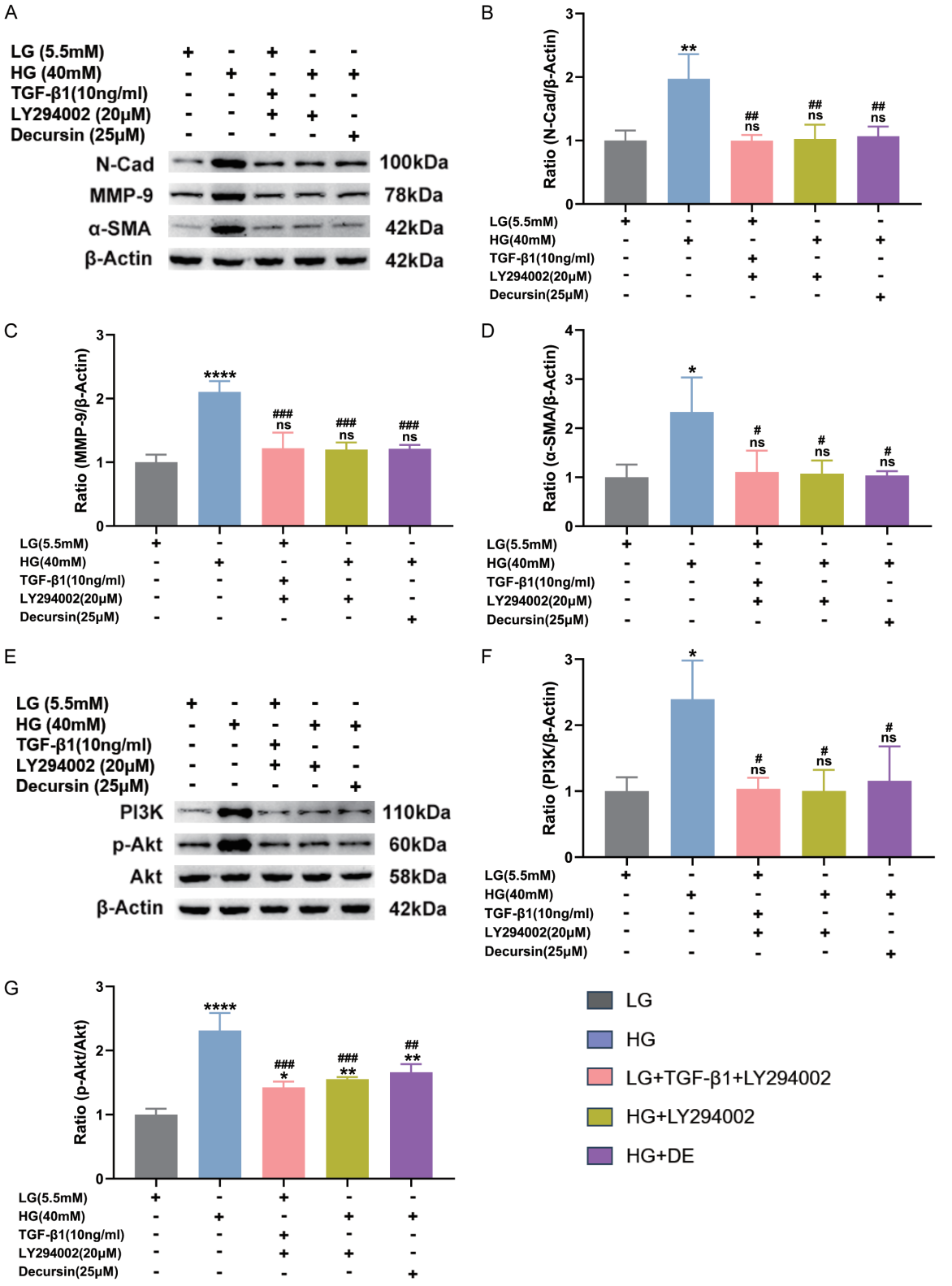

Figure 6. DE alleviates HG-induced EMT in HK2 cells by inhibiting the PI3K/Akt pathway. A. Western blotting images of N-cadherin, MMP-9, and α-SMA in HK2 cells treated as indicated. B-D. Quantitative analysis of N-cadherin, MMP-9, and α-SMA protein levels. E. Representative Western blot images of PI3K, p-Akt, and Akt. F, G. Quantitative analysis of PI3K protein level and the p-Akt/Akt ratio. Data are presented as mean ± SD from three independent experiments (n=3). Statistical significance was determined by one-way ANOVA with post-hoc comparisons using GraphPad Prism 9.0. *P < 0.05, **P < 0.01, ****P < 0.0001 versus the LG group; #P < 0.05, ##P < 0.01, ###P < 0.001 versus the HG group. ns, not significant. LG, low-glucose; HG, high glucose; EMT, epithelial-mesenchymal transition; DE, Decursin.

Discussion

In this study, the STZ-induced DKD rat model was employed, primarily based on the following considerations. Firstly, this model enables the rapid and reliable induction of a stable and controllable hyperglycemic state, accompanied by significant pathological features of DKD, such as increased proteinuria, glomerular hypertrophy, and interstitial fibrosis [33]. Secondly, studies have indicated that renal hypertrophy - marked by increased kidney weight and a transition from hyperplastic to hypertrophic growth - occurs in the early stages of STZ-induced diabetic rats [34, 35]. Furthermore, the STZ-induced model offers advantages including a short experimental cycle, cost-effectiveness, and high phenotypic reproducibility, making it a well-established and widely used classic model in DKD pathological mechanism and therapeutic intervention research [36]. Consequently, utilizing this STZ-induced DKD rat model, we observed that four weeks post-modeling, the urinary UACR, BUN, and KW/BW were significantly elevated in DKD model rats, which is consistent with previous findings. An increased UACR is a characteristic feature of DKD. Following 12 weeks of DE administration, UACR and BUN were significantly reduced; however, no significant change was observed in KW/BW, a phenomenon that may be associated with established renal fibrosis. Fibrosis, particularly driven by the EMT process, is a central pathological manifestation of diabetic nephropathy [37]. Our results demonstrated that DE not only attenuated renal tubular hypertrophy and glomerular enlargement but also reduced the accumulation of glycogen and collagen fibers in DKD rats. Therefore, alongside glycemic control, developing therapies that target renal EMT is crucial for mitigating fibrosis and altering the progression of DKD.

DE is a primary active component derived from the roots of *Angelica gigas* Nakai. It has demonstrated therapeutic potential in various pathophysiological conditions, including cancer, inflammation, and neurodegenerative diseases [38, 39]. Moreover, DE has been reported to downregulate the expression and activity of matrix metalloproteinases by modulating p38 phosphorylation [40]. Although the pharmacological properties of DE are well-documented, its anti-fibrotic effect in DKD remains unclear. In this study, we employed network pharmacology and molecular docking to investigate its mechanism of action against renal EMT in DKD. We identified 16 overlapping targets, from which five key targets - MMP-9, ESR1, PTGS2, AR, and CTNNB1 - were prioritized. Molecular docking further predicted strong binding affinity of DE to MMP-9, PI3K, and Akt. These in silico findings provided a foundational rationale for our subsequent experimental validation.

MMP-9, a gelatinase produced by various cell types including epithelial cells and fibroblasts, plays a critical role in renal EMT by degrading the epithelial basement membrane [41]. It can also promote renal interstitial fibrosis via activation of extracellular signal-regulated kinases, while its inhibition attenuates α-SMA expression and ameliorates fibrosis [42, 43]. TGF-β1 and high glucose are established major inducers of EMT in renal fibrosis [44]. In line with this, our study showed that HG treatment significantly upregulated the expression of EMT-related proteins (MMP-9, α-SMA, and N-cadherin) in HK2 cells, mirroring the effect of TGF-β1. DE treatment effectively reversed these HG-induced elevations. Notably, DE also significantly decreased the levels of these proteins in the kidneys of DKD rats. These results confirm that EMT constitutes a key therapeutic target of DE in DKD.

The PI3K/Akt signaling pathway is critically involved in the fibrotic pathogenesis of DKD [26]. Under diabetic conditions, this pathway, which regulates cell growth and EMT, becomes activated in renal tubular epithelial cells [45].

Evidence suggests that PI3K/Akt activation can initiate EMT and promote cellular proliferation and invasion [46]. The PI3K inhibitor LY294002 has been shown to prevent HG-induced EMT by suppressing Akt phosphorylation in renal cells [47]. However, whether the anti-EMT effect of DE involves the PI3K/Akt pathway was previously unknown. Our findings revealed that DE significantly inhibited the activation of the PI3K/Akt pathway in DKD rat kidneys. In vitro, DE markedly reduced HG-induced PI3K/Akt activation in HK2 cells, an effect comparable to that of LY294002. Therefore, we conclude that inhibition of the PI3K/Akt pathway is a key mechanism through which DE mitigates EMT.

This study has several limitations. First, although we demonstrated that DE inhibits PI3K/Akt signaling and thereby ameliorates renal EMT, the specific upstream regulators (e.g., specific transcription factors or miRNAs) of this pathway within the context of DKD and DE treatment were not explored. Second, While the present study demonstrates that DE directly inhibits EMT in renal tubular epithelial cells, the amelioration of renal fibrosis likely involves multicellular crosstalk. Future studies should explore whether DE also modulates the activation, migration, or secretory functions of mesenchymal stromal cells, which may further contribute to its anti-fibrotic effects. Furthermore, the STZ-induced DKD rat model used primarily mimics the pathological features of type 1 diabetes, which differs in etiology from the more prevalent type 2 diabetic nephropathy characterized by multiple metabolic disturbances in the clinical setting; moreover, its fibrotic progression is relatively singular. Additionally, regarding mechanistic validation, while we employed a PI3K inhibitor for reverse confirmation, we were unable to perform a complementary functional rescue experiment using a PI3K agonist to more completely establish the causal chain. Therefore, more comprehensive mechanistic studies are warranted to fully elucidate the anti-fibrotic actions of DE. Finally, investigating the therapeutic potential of DE as a monotherapy or in combination with standard anti-diabetic agents represents a valuable direction for future research.

Conclusions

In summary, the predictions from network pharmacological regarding the targets and pathways of DE in DKD treatment were validated by our subsequent in vitro and animal experiments. Our results suggested that DE alleviates EMT in DKD rats, and the underlying mechanism is associated with the downregulation of PI3K expression and Akt phosphorylation.

Overall, these findings provide important insights into the antifibrotic effects of DE in DKD. Furthermore, DE ameliorated dyslipidemia in DKD rats. Collectively, our study offers a theoretical basis for the clinical translation of DE as a potential therapeutic agent for DKD.

Acknowledgements

This study was supported by Kunming Medical University Joint Special Project - General Program (202001AY070001-091); and the National Natural Science Foundation of China (81760734).

Disclosure of conflict of interest

None.

Abbreviations

EMT, epithelial-mesenchymal transition; DKD, diabetic kidney disease; DE, Decursin; PI3K, phosphatidylinositol 3-kinase; Akt, protein kinase B; UACR, urine albumin to creatinine ratio; KW/BW, kidney weight-to-body weight ratio; BUN, blood urea nitrogen; UA, urea acid; SCr, serum creatinine; TC, total cholesterol; TG, triglyceride; TCMSP, traditional Chinese medicine systems pharmacology database and analysis platform; STITCH, search tool for interacting chemicals; TTD, therapeutic target database; OMIM, online Mendelian inheritance in man; PPI, protein-protein interaction; MMP-9, matrix metallopeptidase 9; PGTS2, prostaglandin-endoperoxide synthase 2; AR, androgen receptor; ESR1, estrogen receptor alpha; CTNNB1, catenin beta 1; LG, low glucose medium; HG, high glucose medium; α-SMA, alpha-smooth muscle actin.

Address correspondence to: Ke Yang, Ruijin Hospital Shanghai Jiaotong University School of Medicine, Shanghai, China. E-mail: ykk_ykkk@126.com; Ying Yang, Department of Endocrinology, Kunming Medical University, The Affiliated Hospital of Yunnan University, Kunming, Yunnan, China. E-mail: YY_2072@126.com

References

[1] Fineberg D, Jandeleit-Dahm KA and Cooper ME. Diabetic nephropathy: diagnosis and treatment. Nat Rev Endocrinol 2013; 9: 713-723.

[2] Huang S, Xu Y, Ge X, Xu B, Peng W, Jiang X, Shen L and Xia L. Long noncoding RNA NEAT1 accelerates the proliferation and fibrosis in diabetic nephropathy through activating Akt/mTOR signaling pathway. J Cell Physiol 2019; 234: 11200-11207.

[3] Anders HJ, Huber TB, Isermann B and Schiffer M. CKD in diabetes: diabetic kidney disease versus nondiabetic kidney disease. Nat Rev Nephrol 2018; 14: 361-377.

[4] Global, regional, and national age-sex-specific mortality for 282 causes of death in 195 countries and territories, 1980-2017: a systematic analysis for the Global Burden of Disease Study 2017. Lancet 2018; 392: 1736-1788.

[5] Dasgupta I and Singh AK. Review: In diabetes, intensive and standard glycemic control do not differ for end-stage kidney disease or death. Ann Intern Med 2017; 167: Jc47.

[6] Nathan DM. Realising the long-term promise of insulin therapy: the DCCT/EDIC study. Diabetologia 2021; 64: 1049-1058.

[7] Lin YC, Chang YH, Yang SY, Wu KD and Chu TS. Update of pathophysiology and management of diabetic kidney disease. J Formos Med Assoc 2018; 117: 662-675.

[8] Lovisa S, LeBleu VS, Tampe B, Sugimoto H, Vadnagara K, Carstens JL, Wu CC, Hagos Y, Burckhardt BC, Pentcheva-Hoang T, Nischal H, Allison JP, Zeisberg M and Kalluri R. Epithelial-to-mesenchymal transition induces cell cycle arrest and parenchymal damage in renal fibrosis. Nat Med 2015; 21: 998-1009.

[9] Li Y, Hu Q, Li C, Liang K, Xiang Y, Hsiao H, Nguyen TK, Park PK, Egranov SD, Ambati CR, Putluri N, Hawke DH, Han L, Hung MC, Danesh FR, Yang L and Lin C. PTEN-induced partial epithelial-mesenchymal transition drives diabetic kidney disease. J Clin Invest 2019; 129: 1129-1151.

[10] Tuleta I and Frangogiannis NG. Diabetic fibrosis. Biochim Biophys Acta Mol Basis Dis 2021; 1867: 166044.

[11] Mohandes S, Doke T, Hu H, Mukhi D, Dhillon P and Susztak K. Molecular pathways that drive diabetic kidney disease. J Clin Invest 2023; 133: e165654.

[12] Wang Z, Chen Z, Li B, Zhang B, Du Y, Liu Y, He Y and Chen X. Curcumin attenuates renal interstitial fibrosis of obstructive nephropathy by suppressing epithelial-mesenchymal transition through inhibition of the TLR4/NF-κB and PI3K/AKT signalling pathways. Pharm Biol 2020; 58: 828-837.

[13] Shin JH, Kim KM, Jeong JU, Shin JM, Kang JH, Bang K and Kim JH. Nrf2-heme oxygenase-1 attenuates high-glucose-induced epithelial-to-mesenchymal transition of renal tubule cells by inhibiting ROS-mediated PI3K/Akt/GSK-3β signaling. J Diabetes Res 2019; 2019: 2510105.

[14] Dou F, Liu Y, Liu L, Wang J, Sun T, Mu F, Guo Q, Guo C, Jia N, Liu W, Ding Y and Wen A. Aloe-emodin ameliorates renal fibrosis via inhibiting PI3K/Akt/mTOR signaling pathway in vivo and in vitro. Rejuvenation Res 2019; 22: 218-229.

[15] Hu H, Hu S, Xu S, Gao Y, Zeng F and Shui H. miR-29b regulates Ang II-induced EMT of rat renal tubular epithelial cells via targeting PI3K/AKT signaling pathway. Int J Mol Med 2018; 42: 453-460.

[16] Sowndhararajan K and Kim S. Neuroprotective and cognitive enhancement potentials of Angelica gigas Nakai root: a review. Sci Pharm 2017; 85: 21.

[17] Reddy CS, Kim SC, Hur M, Kim YB, Park CG, Lee WM, Jang JK and Koo SC. Natural Korean Medicine Dang-Gui: biosynthesis, effective extraction and formulations of major active pyranocoumarins, their molecular action mechanism in cancer, and other biological activities. Molecules 2017; 22: 2170.

[18] Kim WJ, Lee MY, Kim JH, Suk K and Lee WH. Decursinol angelate blocks transmigration and inflammatory activation of cancer cells through inhibition of PI3K, ERK and NF-kappaB activation. Cancer Lett 2010; 296: 35-42.

[19] Yang Y, Yang K, Li Y, Li X, Sun Q, Meng H, Zeng Y, Hu Y and Zhang Y. Decursin inhibited proliferation and angiogenesis of endothelial cells to suppress diabetic retinopathy via VEGFR2. Mol Cell Endocrinol 2013; 378: 46-52.

[20] Zhu ML, Li JC, Wang L, Zhong X, Zhang YW, Tan RZ, Wang HL, Fan JM and Wang L. Decursin inhibits the growth of HeLa cervical cancer cells through PI3K/Akt signaling. J Asian Nat Prod Res 2021; 23: 584-595.

[21] Li L, Zhang J, Xing C, Kim SH and Lü J. Single oral dose pharmacokinetics of decursin, decursinol angelate, and decursinol in rats. Planta Med 2013; 79: 275-280.

[22] Shannon P, Markiel A, Ozier O, Baliga NS, Wang JT, Ramage D, Amin N, Schwikowski B and Ideker T. Cytoscape: a software environment for integrated models of biomolecular interaction networks. Genome Res 2003; 13: 2498-2504.

[23] Morris GM, Huey R, Lindstrom W, Sanner MF, Belew RK, Goodsell DS and Olson AJ. AutoDock4 and AutoDockTools4: Automated docking with selective receptor flexibility. J Comput Chem 2009; 30: 2785-2791.

[24] Trott O and Olson AJ. AutoDock Vina: improving the speed and accuracy of docking with a new scoring function, efficient optimization, and multithreading. J Comput Chem 2010; 31: 455-461.
[25] Xu Z, Jia K, Wang H, Gao F, Zhao S, Li F and Hao J. METTL14-regulated PI3K/Akt signaling pathway via PTEN affects HDAC5-mediated epithelial-mesenchymal transition of renal tubular cells in diabetic kidney disease. Cell Death Dis 2021; 12: 32.
[26] Zhang Y, Jin D, Kang X, Zhou R, Sun Y, Lian F and Tong X. Signaling pathways involved in diabetic renal fibrosis. Front Cell Dev Biol 2021; 9: 696542.
[27] Khan A, Diwan A, Thabet HK, Imran M and Bakht MA. Discovery of novel pyridazine-based cyclooxygenase-2 inhibitors with a promising gastric safety profile. Molecules 2020; 25: 2002.
[28] Garmaa G, Manzéger A, Haghighi S and Kökény G. HK-2 cell response to TGF-β highly depends on cell culture medium formulations. Histochem Cell Biol 2024; 161: 69-79.
[29] Ge A, Ma Y, Liu YN, Li YS, Gu H, Zhang JX, Wang QX, Zeng XN and Huang M. Diosmetin prevents TGF-β1-induced epithelial-mesenchymal transition via ROS/MAPK signaling pathways. Life Sci 2016; 153: 1-8.
[30] Liu Y. Epithelial to mesenchymal transition in renal fibrogenesis: pathologic significance, molecular mechanism, and therapeutic intervention. J Am Soc Nephrol 2004; 15: 1-12.
[31] Zheng M, Lv LL, Cao YH, Zhang JD, Wu M, Ma KL, Phillips AO and Liu BC. Urinary mRNA markers of epithelial-mesenchymal transition correlate with progression of diabetic nephropathy. Clin Endocrinol (Oxf) 2012; 76: 657-664.
[32] Torsello B, De Marco S, Bombelli S, Cifola I, Morabito I, Invernizzi L, Meregalli C, Zucchini N, Strada G, Perego RA and Bianchi C. High glucose induces an activated state of partial epithelial-mesenchymal transition in human primary tubular cell cultures. PLoS One 2023; 18: e0279655.
[33] Zhou Y, Lou C, Xu X, Feng B, Fan X and Wang X. Ursolic acid ameliorates diabetic nephropathy by inhibiting JAK2/STAT3-driven ferroptosis: mechanistic insights from network pharmacology and experimental validation. Drug Des Devel Ther 2025; 19: 6699-6717.
[34] Huang HC and Preisig PA. G1 kinases and transforming growth factor-beta signaling are associated with a growth pattern switch in diabetes-induced renal growth. Kidney Int 2000; 58: 162-172.
[35] Bak M, Thomsen K, Christiansen T and Flyvbjerg A. Renal enlargement precedes renal hyperfiltration in early experimental diabetes in rats. J Am Soc Nephrol 2000; 11: 1287-1292.
[36] Pointeau O, Barbosa R, Loriot M, Leemput J, Dubus E, Causse SZ, Demizieux L, Passilly-Degrace P, Degrace P, Vergès B and Jourdan T. A simplified and robust model for the study of diabetic nephropathy: streptozotocin-induced diabetic mice fed a high-protein diet. Int J Mol Sci 2025; 26: 2477.
[37] Tang SC, Yiu WH, Lin M and Lai KN. Diabetic nephropathy and proximal tubular damage. J Ren Nutr 2015; 25: 230-233.
[38] Lee TK, Kang IJ, Sim H, Lee JC, Ahn JH, Kim DW, Park JH, Lee CH, Kim JD, Won MH and Choi SY. Therapeutic effects of Decursin and Angelica gigas Nakai root extract in gerbil brain after transient ischemia via protecting BBB leakage and astrocyte endfeet damage. Molecules 2021; 26: 2161.
[39] Choi YJ, Kim DH, Kim SJ, Kim J, Jeong SI, Chung CH, Yu KY and Kim SY. Decursin attenuates hepatic fibrogenesis through interrupting TGF-beta-mediated NAD(P)H oxidase activation and Smad signaling in vivo and in vitro. Life Sci 2014; 108: 94-103.
[40] Kweon B, Han YH, Kee JY, Mun JG, Jeon HD, Yoon DH, Choi BM and Hong SH. Effect of angelica gigas Nakai ethanol extract and Decursin on human pancreatic cancer cells. Molecules 2020; 25: 2028.
[41] Yang J, Shultz RW, Mars WM, Wegner RE, Li Y, Dai C, Nejak K and Liu Y. Disruption of tissue-type plasminogen activator gene in mice reduces renal interstitial fibrosis in obstructive nephropathy. J Clin Invest 2002; 110: 1525-1538.
[42] Tan TK, Zheng G, Hsu TT, Lee SR, Zhang J, Zhao Y, Tian X, Wang Y, Wang YM, Cao Q, Wang Y, Lee VW, Wang C, Zheng D, Alexander SI, Thompson E and Harris DC. Matrix metalloproteinase-9 of tubular and macrophage origin contributes to the pathogenesis of renal fibrosis via macrophage recruitment through osteopontin cleavage. Lab Invest 2013; 93: 434-449.
[43] Tan TK, Zheng G, Hsu TT, Wang Y, Lee VW, Tian X, Wang Y, Cao Q, Wang Y and Harris DC. Macrophage matrix metalloproteinase-9 mediates epithelial-mesenchymal transition in vitro in murine renal tubular cells. Am J Pathol 2010; 176: 1256-1270.
[44] Song S, Qiu D, Luo F, Wei J, Wu M, Wu H, Du C, Du Y, Ren Y, Chen N, Duan H and Shi Y. Knockdown of NLRP3 alleviates high glucose or TGFB1-induced EMT in human renal tubular cells. J Mol Endocrinol 2018; 61: 101-113.
[45] Lei L, Zhao J, Liu XQ, Chen J, Qi XM, Xia LL and Wu YG. Wogonin alleviates kidney tubular epithelial injury in diabetic nephropathy by inhibit-

ing PI3K/Akt/NF-κB signaling pathways. Drug Des Devel Ther 2021; 15: 3131-3150.
[46] Tian K, Du G, Wang X, Wu X, Li L, Liu W and Wu R. MMP-9 secreted by M2-type macrophages promotes Wilms' tumour metastasis through the PI3K/AKT pathway. Mol Biol Rep 2022; 49: 3469-3480.
[47] Lu Q, Wang WW, Zhang MZ, Ma ZX, Qiu XR, Shen M and Yin XX. ROS induces epithelial-mesenchymal transition via the TGF-β1/PI3K/Akt/mTOR pathway in diabetic nephropathy. Exp Ther Med 2019; 17: 835-846.

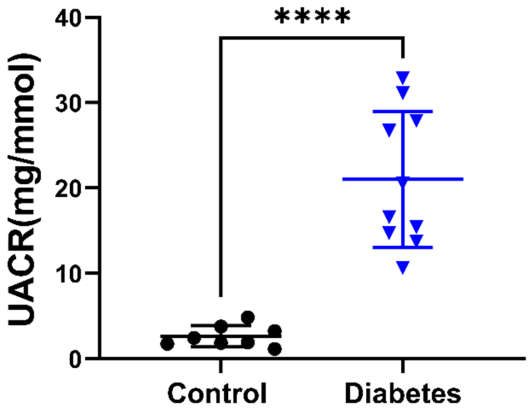

Supplementary Figure 1. The change of UACR in Control and Diabetes rat groups after STZ injection for 4 weeks. Data are expressed as the mean ± SD. Statistical significance of differences were confirmed by Student t-test using GraphPad Prism 9.0 software. ****P < 0.0001. Control, normal rats' group (n=8); Diabetes, diabetic rats' group (n=10 randomly). UACR, urinary albumin-to-creatinine ratio.

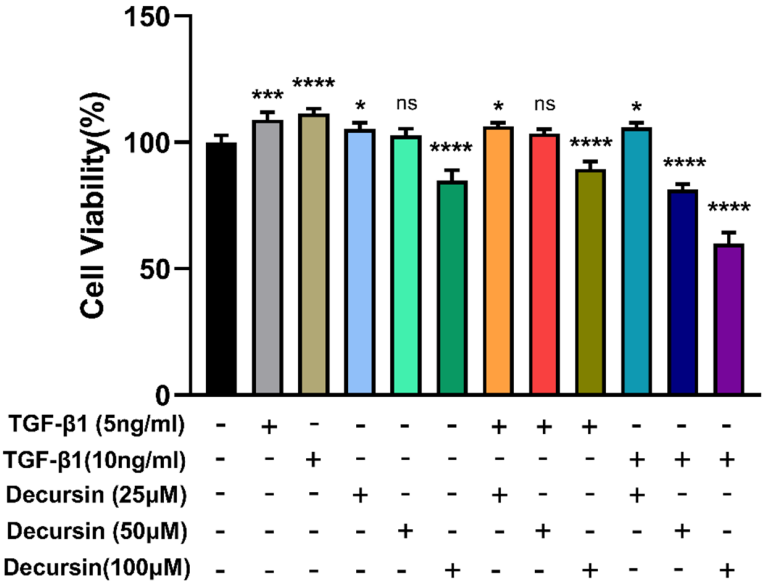

Supplementary Figure 2. MTS assay of DE on HK2 cells viability. HK2 cells were treated with different concentrations of DE and TGF-β1. Data are expressed as the mean ± SD. Data were obtained from three independent experiments. Statistical significance of the differences were confirmed by one-way ANOVA using GraphPad Prism 9.0 software. ns: no statistical significance, *P < 0.05, **P < 0.01, ***P < 0.001, ****P < 0.0001, vs. the control group. DE, Decursin.

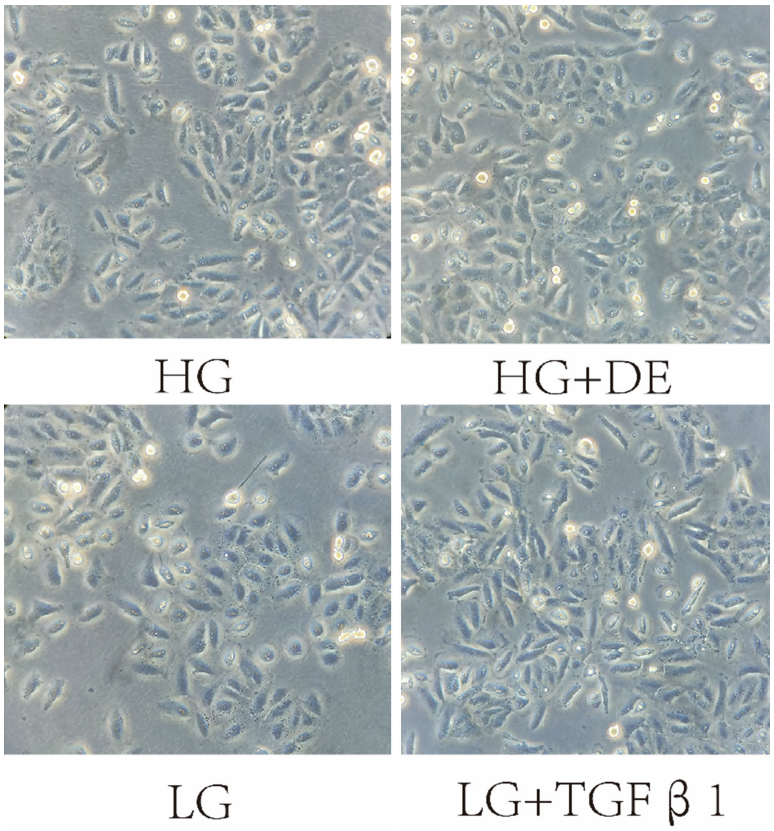

Supplementary Figure 3. DE improved HG-induced HK2 cells shape. Compared with LG-treated HK2 cells, HG could induce most HK2 cells to exhibit a long spindle-like shape, the same phenotype as TGF-β1 induced. After Decursin treatment, the appearance of HK2 cells was greatly improved, and most of them were in the original pebble-like shape. LG, low-glucose; HG, high glucose; DE, Decursin.